Journal of Asian Concrete Federation
Vol. 8, No. 1, pp. 26-36, June. 2022
ISSN 2465-7964 / eISSN 2465-7972
DOI http://dx.doi.org/10.18702/acf.2022.6.8.1.26

Technical Paper

A Case Study on Condition Assessment of Fire-Damaged RC Members of Turbo-Generator

Sanjay Mundra*, TVG Reddy, Nitesh Kumar, Shivang Bansal, P N Ojha

(Received: February 02, 2022; Accepted: March 03, 2022; Published online: June 30, 2022)

Abstract: Many researchers across the globe have carried out fire safety risk analysis to gather evidence and pertinent data for different Reinforced Cement Concrete (RCC) members exposed to fire. Assessment of fire-damaged structures furnishes the minute details of the effect of fire on the properties of concrete.The study indicates the condition assessment of the turbo-generator (TG) unit, comprises of concrete bearing pedestals, deck and supporting columns. The research was conducted using Non-Destructive Testing (NDT) techniques using Rebound hammer test, Ultrasonic Pulse Velocity (UPV) test, Concrete Cover measurement, Carbonation and Crack depth measurements followed by microstructural studies using an X-ray Diffraction (XRD), Scanning Electron Microscope (SEM), Optical Microscope (OM), and Mercury Intrusion Porosimetry (MIP). The samples were taken from a fire-damaged concrete bearing pedestal B2 and a non-fire-damaged concrete bearing pedestal B4 of the TG unit. The approach enabled us to find the extent of damage to the RCC members exposed to fire. The above mentioned test witnessed that the concrete bearing pedestal B2 was the moderately distressed member, expressed doubtful quality of concrete, higher porosity, reduced residual compressive strength and reduction in yield strength of steel. However minor distress in form of crushing at the top grout portion was observed in concrete bearing pedestal B4, and no apparent distress was observed in supporting columns of TG unit. Based on the distress identified, repair and remedial measures were proposed to concrete bearing pedestals in order to improve the performance of the TG unit.

Keywords: Concrete; Fire damage structure; Non-destructive test; Core Extraction; Microstructure; Repair Methodology

1. Introduction

The severity of fire damage in RCC members of any structure depends upon the period of exposure to fire. An adequate cover should be provided during the design stage to protect the structure from fire. The continual exposure of concrete to elevated temperatures causes physical, chemical and microstructural changes. Fire-damaged concrete increases in contact-type defects result in the degradation of mechanical properties, including stiffness and strength [1]. The fire may cause deterioration of RCC members in the form of spalling, crushing, cracking, loss of cross-section of reinforcement bars, loss of cover, reduction in mechanical strength and changes in concrete microstructure. Xiao. J. et al [2] stated explosive thermal spalling is a catastrophic failure of concrete that generally occurs during a fire and is characterized as explosively breaking into pieces, often without notice as in this case study. Xiao. J et al [3] stated generally concrete spalling occurs in the initial stage of fire, reinforcement bars and internal layers will be exposed to the direct fire. Yenigalla et al [4] tabulated that the activity of fire on RCC structures causes various types of damages ranging from minor colour change, severe cracking and spalling of concrete depending on the intensity of fire. Handoo and

***Corresponding author Sanjay Mundra** *is a General Manager in Construction Development and Research, in Ballabgarh-Haryana, NCB, India.*

TVG Reddy *is a Superintendent Engineer in National Institute of Technology Warangal, India.*

Nitesh Kumar *is a Project Engineer in Construction Development and Research, in Ballabgarh-Haryana, NCB, India.*

Shivang Bansal *is a Project Scientist in Construction Development and Research, in Ballabgarh-Haryana, NCB, India.*

P N Ojha *is a Joint Director in Construction Development and Research, in Ballabgarh-Haryana, NCB, India.*

Agrawal [5], reported the reduction in compressive strength of concrete. The preliminary diagnosis helped to collect the evidence and accidental data to get general information of the exposure period, type of damage, the appearance of surface texture, and change in colour of various RCC members. The information about the type and amount of combustible materials can be used for estimating the probable temperatures reached in buildings [6]. This case study was out situated in North India on a fire damaged TG unit comprising of a deck, concrete bearing pedestal and supporting columns. Based on preliminary studies, the scope of the investigation was finalized which covers visual Inspection, NDT at the field followed by lab research on collected samples. Based on the extent of damage to the existing structure the repair and re-strengthening were proposed, to improve the performance.

Assessing the extent and gravity of fire damage on RCC structures is a crucial task to plan the rehabilitation or the demolition of their structures [7]. Almost all the available literature underlined that chemically bound water from the calcium silicate hydrate (C-S-H) gel starts dehydrating at 110°C. The dehydration of the hydrated calcium silicate and the thermal expansion of the aggregate increase internal stresses and from 300°C, micro-cracks are induced through the material [8]. Calcium hydroxide dissociates at around 450 to 500°C resulting in concrete shrinkage. Spalling and pop-outs of concrete are confined to surface close to areas exposed to fire, an indicator of heating at 573°C [9]. The decomposition of the hydrated calcium silicate begins around 700°C [10]. Concrete crumbled to gravel by the fingers at 800°C, whereas at 1150°C and above the minerals of the cement paste turn into a glass phase [11].

The TG unit (500 MW capacity) was constructed in the year 2012 as shown in Figure 1. The incidence of fire occurred in the year 2019 on the TG deck slab and surrounding bearing pedestals for 2 hours, followed by the impact of turbo generator assemblies on RCC members and structural steel sections in the turbine area. Investigations were carried out on the fire-damaged concrete bearing pedestals, TG deck slab, and supporting columns. The detailed visual inspection, distress mapping and extent of damage to structural elements was carried out to access the structural integrity.

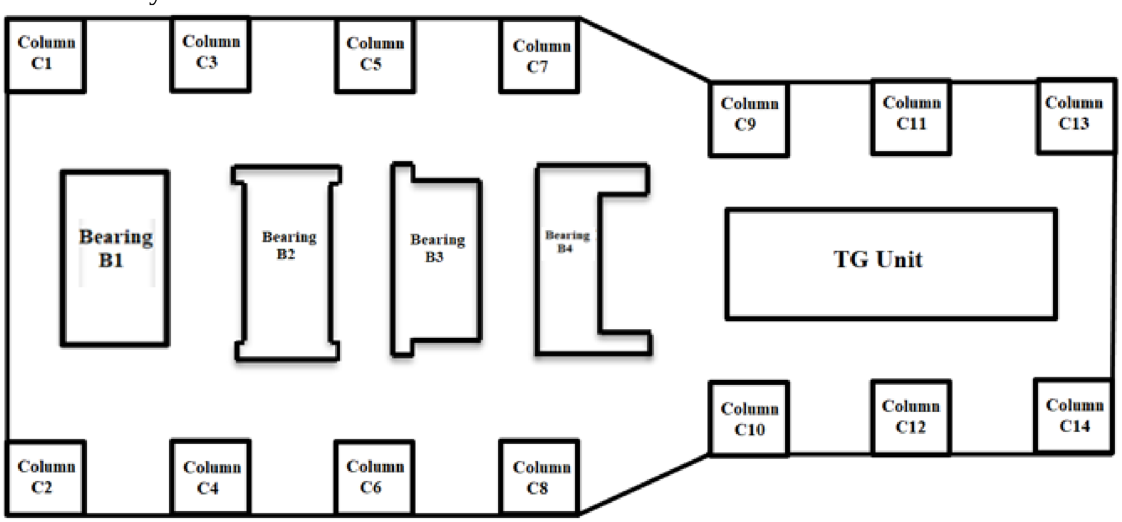

Fig. 1 – Typical Sketch of TG unit with concrete bearing pedestals and supporting column

2. Experimental Plan

The complete study is divided into four phases which are reported as under:

Phase-1: Preliminary Site inspection (inspection after exposure of fire)

- Source of fire, and the fire exposure period
- Fire damaged locations and types of damage – no apparent distress, minor distress and moderate stress category
- Surface texture, change in colour, soundness of concrete and visible cracks on the surface
- Collection of structural drawings and records

Phase-2: In-situ detailed investigation

- Visual Inspection

- Ultrasonic pulse velocity measurements on RCC members
- Rebound hammer test
- Cover measurements and Core extraction test
- Crack depth/Width measurements
- Carbonation depth measurements
- Mechanical properties of Rebar Samples

Phase-3: Microstructural and Chemical investigation in the laboratory

- Scanning electron microscopy (SEM)
- X-ray Diffraction (XRD) technique
- Optical Microscopy (OM)
- Mercury Intrusion Porosimetry (MIP)

Phase- 4: Interpretation and Report Preparation

- Interpretation of test results
- Conclusions
- Recommendations for repair and re-strengthening measures

3. Results and Discussion

3.1 Preliminary site Inspection

In phase-1, preliminary inspection data was collected along with photographs. As per information collected from eyewitnesses present during a fire, the fire was initiated near concrete bearing pedestal B2 and the dousing of the same was done within 2 hours. The surface of concrete bearing pedestals showed a change in colour from grey to blackish-grey along with deposition of soot. Spalling and crushing were also observed at the top portion of the concrete bearing pedestal. The information extracted from the structural drawings indicated that the grade of concrete and grade of reinforcement was M 35 and Fe 500 respectively.

3.2 Detailed investigation

Phase-2 comprises of visual observations along with non-destructive testing at identified locations as mentioned below:

3.2.1 Visual Inspection

The visual inspection indicated the crushing and spalling of top grout and underneath concrete was observed at concrete bearing pedestals of B2 and B4 (as shown in Figure 2 and Figure 3). The crack width and depth were measured by using a crackoscope and UPV equipment, respectively. In addition to soot, inclined cracks initiated from the top and extended to downward direction were also observed on concrete bearing pedestal B2 (width varies from 0.25 to 0.4 mm, depth varies from 73 to 112 mm, and length of approx. 350 mm). No such cracks were observed on concrete bearing pedestal B4. Deposition of soot on a small portion of the deck slab soffit was also observed. However, no deposition of soot and change in colour were observed at supporting columns. Side and top reinforcement were exposed at a few locations on a pedestal bearing B2. Change in colour from grey to black was observed on cores extracted from concrete bearing pedestal B2 as shown in Figure 4 and Figure 5. Based on the visual inspection it was observed that concrete bearing pedestal B2 was moderately distressed while pedestal B4 and deck slab were in the minor distress category and no apparent distress was observed on supporting columns.

Fig. 2 – Spalling and crushing of top chemical grout along with underneath concrete and black stains of the fire-damaged face of Pedestal B2

Fig.3 – Spalling and crushing of top chemical grout of Pedestal B4

Fig. 4 – Extraction of cores from the concrete bearing pedestal B-2

Fig. 5 – Colour change to a blackish grey colour in the cover region of concrete bearing pedestal B2.

3.2.2 Ultrasonic Pulse Velocity Measurements

Ultrasonic Pulse Velocity measurements were carried out by the cross-probing method at different locations as per IS 516: Part 5: Sec 1: 2018 [12] to assess the quality of concrete in RCC members of the TG unit. The average results of the UPV test on pedestal B2 and B4 were found to be 3.34 km/s and 3.79 km/s, respectively, which indicates that the overall quality of concrete was found to be doubtful in bearing pedestal B2 and good in bearing pedestal B4. The same was supported by Kore et al [13] that there was a decrease in UPV results of fire exposed members. For deck slab and supporting columns, the results were found to be 3.98 km/sec and 4.28 km/sec, respectively, which indicates the overall quality of concrete was good.

3.2.3 Rebound Hammer Test

The test was performed using N-type mechanical rebound hammer as per IS 13311: Part 2: 1992 [14] to predict the likely compressive strength of the fire and non-fire damaged members of the TG unit. The results obtained by Rebound Hammer testing on fire damage concrete bearing pedestal B2 (as shown in Figure 7) indicate the average likely compressive strength of 40.54 MPa, and for non-fire damaged concrete bearing pedestal, i.e., B4 likely compressive strength is 54.92 MPa. The rebound hammer test on other non-fire damage RCC members (TG deck slab and supporting columns) indicates 53.35 MPa and 53.32 MPa, respectively. These results show that the rebound test gives less likely compressive strength on the fire-damaged portion than non-fire damaged, and the variation is approximately 26%. Similar results were also observed by Wróblewska J. et al. [15].

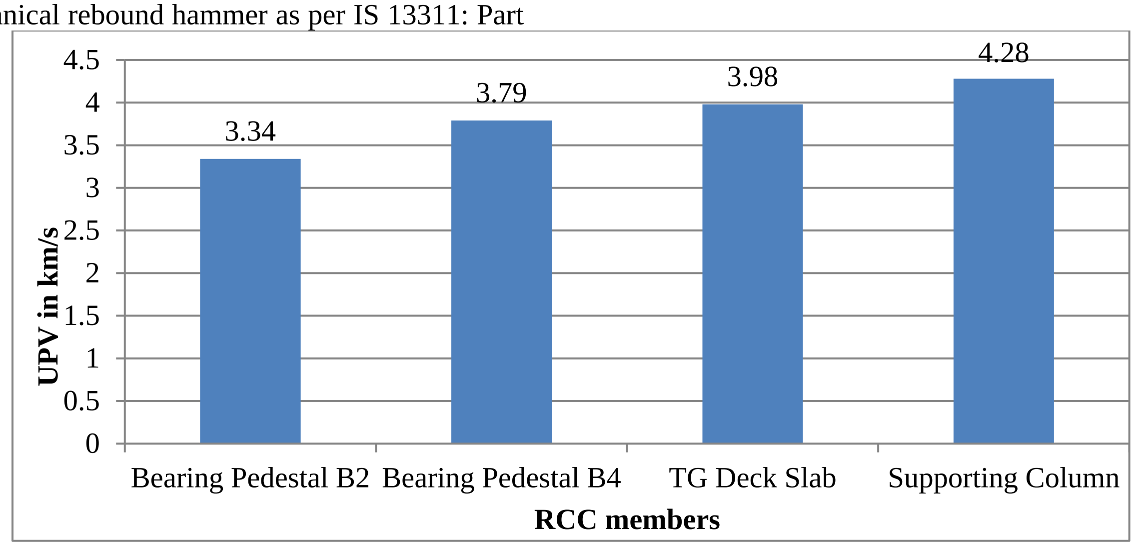

Fig. 6 – UPV (by cross probing method) of various RCC members of the TG unit

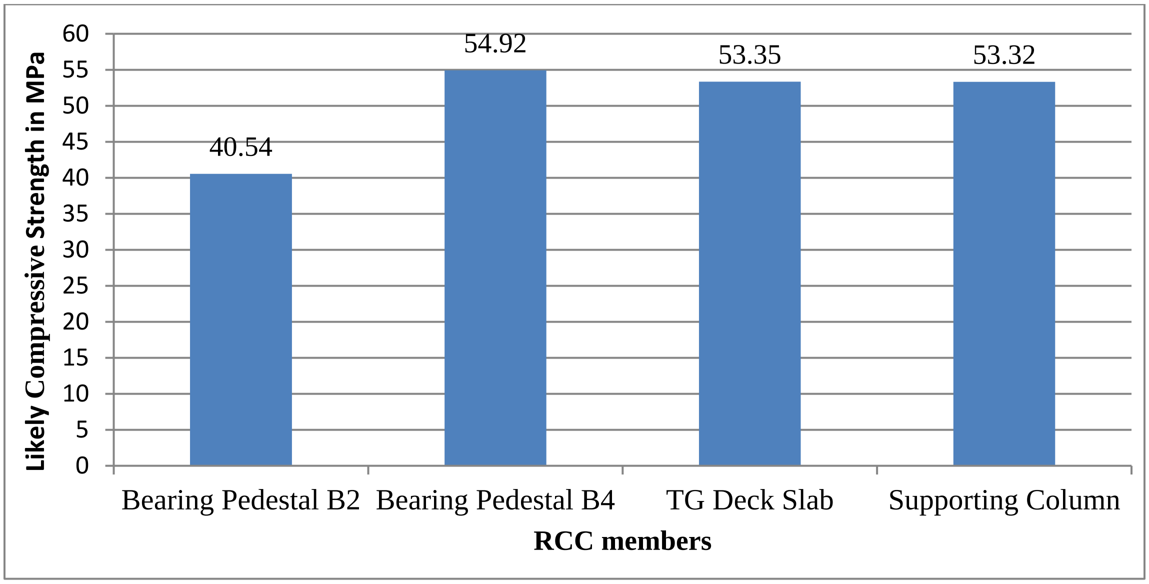

Fig. 7 – Likely Surface Compressive Strength of RCC members of TG unit

3.2.4 Core Sampling and Testing

The cores of 60 mm diameter were extracted from fire-damaged and non-fire damaged locations through a core drilling machine for estimating the compressive strength of in-situ concrete. Its equivalent cube compressive strength was assessed duly by applying the correction factors, i.e., diameter, length/diameter ratio, etc., as per clause 8.4.2 of IS 516: Part 4: 2018 [16]. The average compressive strength of cores extracted from the fire-damaged portion of pedestal B2 and non-fire damaged portion of pedestal B4 were 38.51MPa and 49.67MPa (as shown in Figure 8), respectively. The results are satisfying the requirement of the M 35 grade of concrete. The member exposed to high temperature resulted in a reduction in compressive strength approximately by 22%. Similar trend was observed by Xiao et al [17] for the reduction in residual compressive strength with the increase in temperature. Heating up to 400°C generated relatively small cracks, which did not cause any immediate loss of carrying capacity in compression.

3.2.5 Concrete Cover Measurement

Profoscope instrument was used at identified locations on pedestals B2 and B4 for measuring the concrete cover thickness. The depth of concrete cover to reinforcement steel in the concrete bearing pedestals of B2 and B4 were 25 mm and 33 mm, respectively (shown in Figure 9). The existing concrete cover provided in these concrete bearing pedestals were satisfying the requirement of mild environmental exposure conditions but not meeting the requirement of fire resistance period of 120 minutes as per provisions of table 16 and 16A of IS 456: 2000 [18]. However, at non-fire damaged portions i.e. TG deck slab and columns, both the requirements were satisfied.

3.2.6 Carbonation Depth

The carbonation of concrete is one of the main reasons for the corrosion of reinforcement. The carbonation depth was determined using a pH indicator (solution of 1% phenolphthalein in 70% ethyl alcohol) on extracted concrete cores. The carbonation depth varies from 0 to 5 mm and 5 to 10 mm for the cores extracted from non-fire damaged and fire-damaged concrete bearing pedestal respectively. The depth of carbonation was found to be within the cover region at all identified locations.

3.2.7 Residual Strength of Steel

The residual mechanical properties like ultimate tensile strength (UTS) and yield strength (YS) were determined for reinforced steel specimens extracted from the fire and non-fire affected bearings. The samples extracted from fire-damaged pedestal B2 shows ultimate tensile strength and yield strength of 619 MPa and 493 MPa, respectively. The sample extracted from non-fire damaged pedestal B4 shows ultimate tensile strength and yield strength of 636 MPa and 554 MPa, respectively.

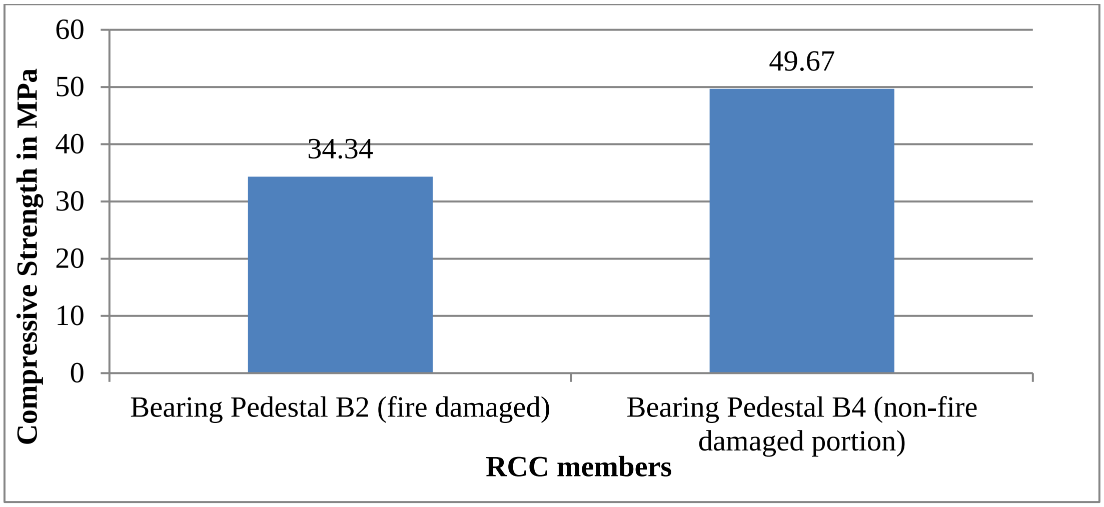

Fig. 8 - Equivalent Cube Compressive Strength of RCC members of TG unit

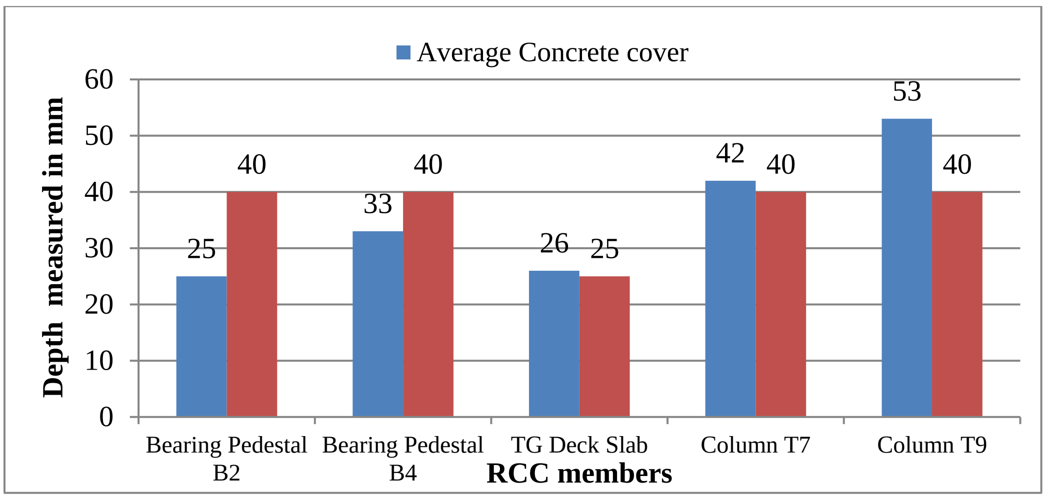

Fig. 9 – Showing Nominal cover requirement as per table 16-A of IS 456: 2000 corresponding to the average concrete cover of RCC members of TG unit

The above results show that the yield strength and ultimate tensile strength of fire and non-fire damaged specimens are comparable. Hence it can be concluded that the maximum temperature during a fire may not have crossed 300^{o}C as there is no significant loss in mechanical strength of steel reinforcement in fire-damaged samples.

3.2.8 Microstructural Investigations

In Phase-3, the microstructural investigation was carried out on 5 mm thick slices obtained from cores to observe the changes in concrete morphology due to fire. As per the test requirements, the representative samples were converted into different forms (powder, chips, etc.).

3.2.9 Scanning electron microscopy (SEM)

In this investigation, the S-400 Scanning Electron Microscope (magnification ranging from 20X to approx. 30,000X, the spatial resolution of 50 to 100 nm) was used to analyse the morphology. The fire-damaged pedestal B2 had shown disturbed or less densified microstructure. Micro-cracks gradually decreased from the depth of 35 mm to 50 mm from 50% to 20% respectively on fire-damaged specimens. The presence of hexagonal crystals was also observed at a depth of 10-15 mm for fire-damaged pedestal B2. The observations for SEM images of bearing pedestal B2 are made in figure 10, where A shows void and cavities due to release of moisture, B shows delayed Ettringite crystal with hair-like projections, C shows the presence of extending cracks [19], which indicates temperature may not cross beyond 350^{o}C. The densified microstructure with Lath-shaped crystals is observed at a depth of 25-30 mm on a non-fire damaged bearing pedestal B4 sample. The observations for SEM images of pedestal B4 are made in figure 11, where D shows dense packing of concrete matrix, E shows grainy filling of cement hydrated particles present in the concrete matrix of cement, F shows filled concrete matrix in void showing cement bound. The presence of Lath-shaped crystals suggests that the presence of ettringite or monosulphoaluminate minerals. These crystals are stable below 150℃ of temperature.

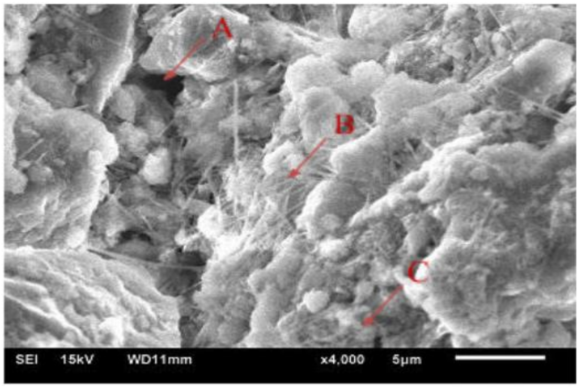

Fig. 10 – SEM micrograph of a sample taken from Concrete bearing pedestal B2 at 30-35mm depth having a relatively loose microstructur**e**

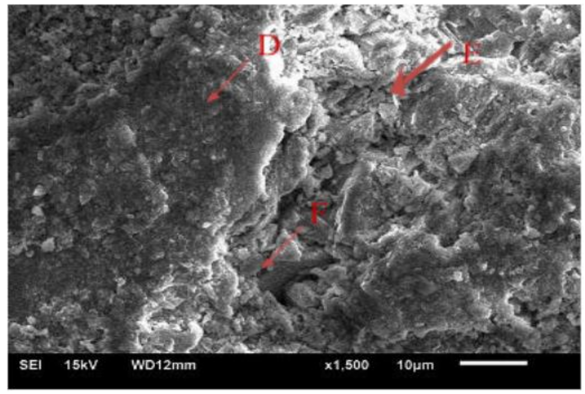

Fig. 11 – SEM micrograph of a sample taken from Concrete bearing pedestal B4 at 25-30mm depth having relatively Densified microstructure

3.2.10 X-Ray Diffraction (XRD)

X-ray diffraction is a popular material characterization technique. This study was carried out to view the effect of elevated temperature on mineralogical changes in hydrated cement paste. The XRD images enable identifying the reduction of portlandite and larnite as depth increases if the concrete is exposed to fire [19]. In the present study, concrete slices at varying depths from the extracted concrete cores were prepared. The mortar/paste portion was ground into fine powder. The XRD patterns (shown in Figure 12 and Figure 13) were generated through powdered samples in the laboratory by using the X-Ray Diffraction technique (PANALYTICAL Expert Pro Powdered diffractometer with Copper Electrode and Ni Filter). In all samples of the bearing pedestal B2 and B4 across various depths, quartz was found to be in abundance along with other phases of feldspar, calcite and dolomite. In fire-damaged pedestal B2, portlandite was found at a depth of 10-15 mm, while in non-fire damaged pedestal B4, the same was found at 5-10 mm depth. This indicates the attended temperature may not have gone beyond 450 to 500°C from the above-mentioned depths in the pedestals.

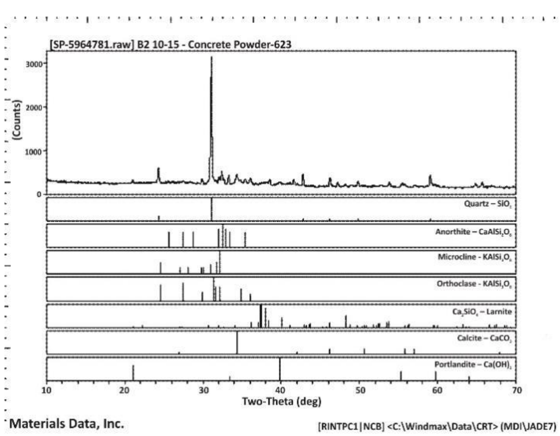

Fig. 12 – XRD peak pattern for 10-15mm depth of Concrete bearing pedestal B2

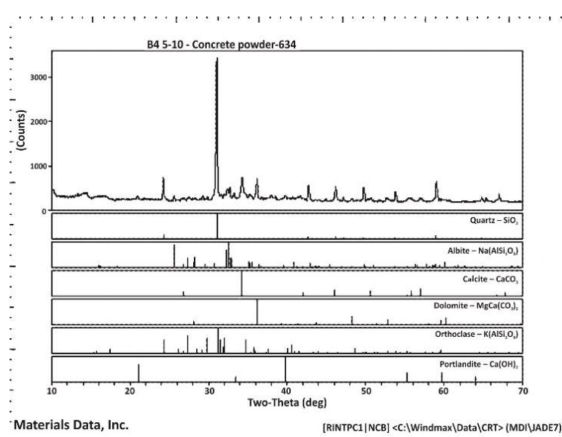

Fig. 13 – XRD peak pattern for 5-10mm depth of Concrete bearing pedestal B4

3.2.11 Mercury Intrusion Porosimetry (MIP)

Mercury Intrusion Porosimetry (MIP) is a powerful technique used to determine porosity, pore size distribution, and pore volume to characterize a wide variety of solid and powdered materials. The test was performed on broken chips of concrete samples collected from both bearing pedestal B2 (fire damaged) and B4 (non-fire damaged) obtained at depth 5-10 mm. The procedure given in ISO 15901-1: 2016 [20] was followed for the test. The results are shown in Table-1.

Table -1 MIP Results

Concrete	Relative Porosity(%)	Pore Volume(mm3/g)	Average pore size(nm)
Pedestal B2 (fire damaged)	13.45	59.71	85.37
Pedestal B4 (non-fire damaged)	10.68	14.57	16.69

It is evident from the results that all the MIP parameters i.e. relative porosity, pore-volume, and the average pore size is higher for fire-damaged concrete sample when compared to the non-fire damaged sample [21]. The possible reason was the disintegration of CSH gel in concrete near the surface in B2, which is also observed in the SEM images. Pore size distribution of both B2 and B4 concrete bearing pedestal at 5-10 mm depth is shown in Figure 14 and Figure 15. However, at a depth of 0-5 mm, the pore volume of concrete bearing pedestal B2 (fire damaged), is found to be less than that of the non-fire damaged pedestal, this may be due to the incidence of burning off some lubricant and burnt particles got stuck on the outer face of the concrete bearing pedestal B2, resulting in a reduction of pore size and volume.

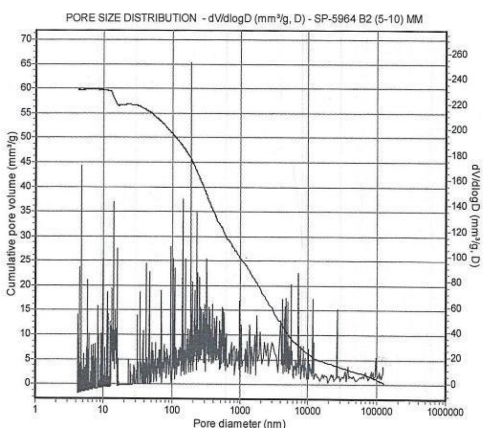

Fig. 14 – Pore size distribution at a depth of 5-10mm of concrete bearing pedestal B2 (fire damaged)

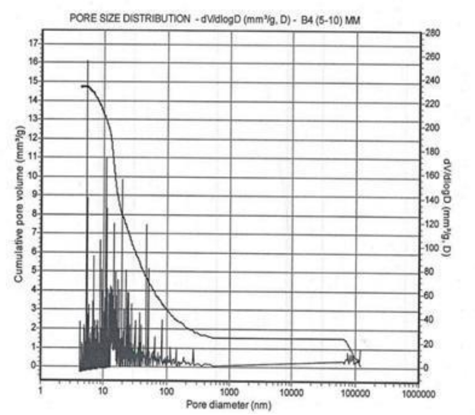

Fig. 15 – Pore size distribution at a depth of 5-10mm of concrete bearing pedestal B4 (non-fire damaged)

3.2.12 Microstructure studies using Stereo-zoom Microscope

The stereo-zoom microscope (SMZ-1500) with Nikon Image system was used to observe the concrete samples extracted from different depths (shown as Figure 16 & Figure 17). The sample taken at a depth of 0-5 mm from fire-damaged bearing pedestal B2 shows that the concrete colour had changed to blackish-grey with a significant number of micro-cracks and partially oxidized fine aggregate. While in non-fire damaged concrete bearing pedestal B4 at a depth of 0-5 mm, the presence of partially closed voids with relatively smooth margins were observed. Microscopic observations also showed significant parallel cracking toward the core axis in concrete bearing pedestal B2, indicating large-scale internal cracking, which may be due to internal shrinkage caused by overheating followed by rapid cooling due to fire-extinguishing.

Fig. 16 – B2-(0-5mm), Development of the cracked surface with partial oxidation of the fine aggregate

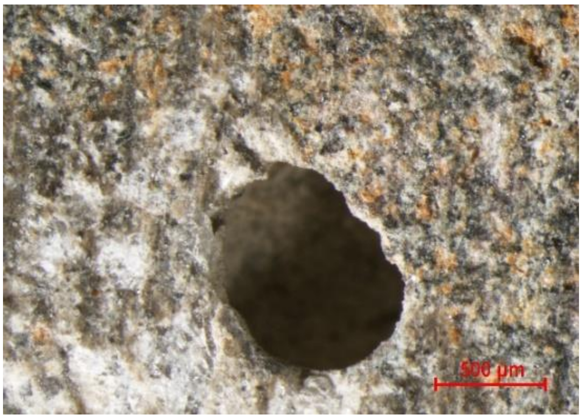

Fig. 17 – B4-(0-5mm), Development of an open void with smooth margins

4. Repair Methodology

The repair methodology proposed based on the results is as follows:

4.1 Grouting: Applied injecting epoxy grout into cracks/honeycomb area using the viscosity of the epoxy grout of fewer than 200 centi-poise.

4.2 Micro-Concrete (Pre-pack): Applied micro-concrete cement-based prepacked single component non-shrink free flow self-compacting in nominal thickness of 100 mm for concrete repair with compressive strength of 35 MPa at 28 Days.

4.3 FRP Wrapping (Double wrap): Applied for strengthening of RCC members with non-metallic composite fibre wrapping system comprising of uni-directional E - glass fibre (900 or similar GSM) and compatible epoxy saturate, by wet layup system.

4.4 Protective coating on repaired and unrepaired surface areas: Applied two or more coats of ready mixed UV resistant and single component acrylic polymer-based waterproofing anti-carbonation coating over a coat of silane siloxane. A total dry film thickness (DFT) including primer will be 225-240 microns.

5. Conclusions

Based on the investigation and interpretation of test results, it is concluded that the concrete bearing pedestal B2 showed a change in colour from grey to blackish-grey along with deposition of soot at the surface. The concrete bearing pedestal B2 was found moderately distressed in the form of spalling, exposed reinforcement and crushing at the top portion, along with several inclined cracks initiated from the top and extended downwards. However, in comparison to concrete bearing pedestal B2, only deposition of soot was observed at few locations of pedestal B4 and was minor distressed. No apparent distress was observed in the TG deck slab and supporting columns.

For both the pedestals, i.e., for fire-damaged B2 and non-fire damaged B4, the compressive strength of concrete was found satisfactory to meet the requirements of the M-35 grade of concrete. Likely Compressive Strength on a fire-damaged concrete pedestal was found lower than that of the non-fire-damaged pedestal. The UPV results indicated that the quality of concrete in non-fire damaged pedestal was good, and it was doubtful for fire-damaged pedestal, due to the formation of internal micro-cracks of concrete.

The presence of portlandite observed by XRD results indicated that the concrete was not exposed to the temperature of 450^{o}C and above as examined from 10-15 mm depth of concrete of fire-damaged pedestal B2 and 5-10 mm depth of non-fire damaged pedestal B4.

From the morphology of SEM images of fire and non-fire damaged pedestal, it was observed that the concrete at a depth of 25-30 mm was dense and not exposed to a temperature of 300^{o}C and above. The portlandite crystals were present at 10-15 mm in fire-damaged pedestal B2 and 5-10 mm depth for non-fire damaged pedestal B4.

Ultimate tensile strength (UTS) and Yield Strength (YS) of reinforcement was found lower for fire damage in comparison to non-fire damage by 3% and 10% respectively.

Further, the repair was proposed for a distressed concrete bearing pedestal using micro concreting at crushed portion followed by FRP wrapping. For inclined cracks, epoxy grouting was proposed. The protective coatings were also suggested for all repaired and non-repaired portions for improving the performance of RC members of the TG unit. This study supports the efficacy of the non-destructive technique to investigate the fire-damaged structures and to evaluate the cause of damage. The study has limitations to chemical analysis which can also be useful parameter to get idea of cause of fire damage through the sample.

Acknowledgements

The authors of this paper would like to express their sincere gratitude to National Council for Cement and Building Materials for providing all the necessary facilities to accomplish this research.

Conflicts of Interest

The authors declare no conflict of interest.

Funding

This research did not receive any specific grant from funding agencies in the public, commercial, or not-for-profit sectors.

References

[1] Park, G.K., and Yim, H. J., (2017). Evaluation of Fire-Damaged Concrete: An Experimental Analysis based on Destructive and Non-destructive Methods, *International Journal of Concrete Structures and Materials*, 11, 447-457.

[2] Xiao J., and Konig G., (2004). Study on concrete at high temperature in China—an overview, *Fire Safety Journal*, 39, 89-103.

[3] Xiao, J., Xie, Q., and Xie, W., (2018). Study on high-performance concrete at high temperatures in China (2004–2016) - An updated overview, *Fire Safety Journal*, 95, 11-24.

[4] Yenigalla R.V., and Sajja, S., (2021). Case Studies on Condition Assessment and Repairs for Fire Damaged Reinforced Cement Concrete Structures, *IOP Conference Series Materials Science and Engineering*, 1112(1), 012022.

[5] Handoo, S.K., and Agarwal, S.K., (2002). Physicochemical, mineralogical, and morphological characteristics of concrete exposed to elevated temperatures, *Cement and Concrete Research*, 32, 1009-1018.

[6] Bernard, E., William, G.H., and William, H.K., (1972). Evaluating fire damage to concrete structures, *Publication#C720154*, The Aberdeen Group.

[7] Stochino, F., Mistretta, F., Meloni, P., and Carcangiu, G., (2017). Integrated approach for post-fire reinforced concrete structures assessment, *Periodica Polytechnica Civil Engineering*, 61(4), 677-699.

[8] Arioz, O., (2007). Effect of elevated temperatures on properties of concrete, *Fire Safety Journal*, 42, 516-522.

[9] Georgali, B., and Tsakiridis, P.E., (2005). Microstructure of fire-damaged concrete, A case study, *Cement and Concrete Composites*, 27(2), 255-259.

[10] Luccioni, B., Figueroa, M., and Danesi, R., (2003). Thermo-mechanic model for concrete exposed to elevated temperatures, *Engineering Structures – Eng Struct*, 25, 729-742.

[11] Hertz, K.D., (2005). Concrete strength for fire safety design, *Magazine of Concrete Research*, 8, 445-453.

[12] IS 516: Part 5: Sec 1: 2018, (2018). Hardened Concrete – Methods of Test Part 5 Non-Destructive Testing of Concrete Section 1 Ultrasonic Pulse Velocity Testing (First Revision), *Bureau of Indian Standards*, New Delhi.

[13] Sudarshan K.D., and Vyas A.K., (2019). Impact of fire on mechanical properties of concrete containing marble waste, *Journal of King Saud University*, 31(1), 42-51.

[14] IS 13311: Part 2: 1992, (1992). Method of Non-destructive Testing of Concrete-methods of Test: Part 2 Rebound Hammer, *Bureau of Indian Standards*, New Delhi.

[15] Wróblewska J., and Kowalski, R., (2020). Assessing concrete strength in fire-damaged structures, *Construction and Building Materials*, 254, 119122.

[16] IS 516: Part 4: 2018, (2018). Hardened Concrete – Methods of Test Part 4 Sampling, Preparing and Testing of Concrete Cores (First Revision), *Bureau of Indian Standards*, New Delhi.

[17] Xiao, j., Li, Z., Xie, Q., and Shen, L., (2016). Effect of strain rate on compressive behaviour of high-strength concrete after exposure to elevated temperatures, *Fire Safety Journal*, 83, 25-37.

[18] IS 456: 2000, (2000). Plain and Reinforced Concrete – Code of Practice, *Bureau of Indian Standards*, New Delhi.

[19] Fernandes, B., Gil, A.M., Bolina, F.L., and Tutikian, B.F., (2016). Assessment of Concrete Exposed to Elevated Temperatures Using Scanning Electron Microscopy and X-Ray Diffraction, *9th International Conference on Structures in Fire*, Princeton.

[20] ISO 15901-1:2016, (2016). Evaluation of pore size distribution and porosimetry of solid materials by mercury porosimetry and gas adsorption, *International Standards Organisation*.

[21] Zhang, Qi., and Ye, G. (2011). Microstructure Analysis of Heated Portland Cement Paste, *Procedia Engineering*, 14, 830-836.